Available online at www.sciencedirect.com
ScienceDirect
Mendeleev Commun., 2020, **30**, 205–208

Mendeleev Communications

Low-valent oligogermanium amidophenolate complex comprising a unique Ge_4 chain

Kseniya V. Tsys,[a] Maxim G. Chegerev,[b] Georgy K. Fukin,[a] Andrey G. Starikov[b] and Alexandr V. Piskunov*[a]

[a] *G. A. Razuvaev Institute of Organometallic Chemistry, Russian Academy of Sciences, 603950 Nizhny Novgorod, Russian Federation. E-mail: pial@iomc.ras.ru*
[b] *Institute of Physical and Organic Chemistry, Southern Federal University, 344090 Rostov-on-Don, Russian Federation*

DOI: 10.1016/j.mencom.2020.03.025

New 10π-electron stabilized O,N-heterocyclic germylene was synthesized and structurally characterized for the first time. Its reduction with potassium in THF resulted in a unique low-valent germanium compound comprising the conjugated Ge_4 chain, which was also characterized by the single crystal X-ray analysis. Bonding aspects in the latter compound have been additionally explored by DFT calculations, which revealed the occurrence of three σ bonds of different (covalent and dative) characters between the Ge atoms.

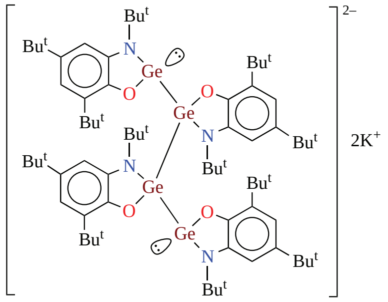

Keywords: germylene, *o*-amidophenolate ligand, low-valent, X-ray, DFT.

Heavier group 14 analogues of carbenes, alkenes, alkynes and dienes have attracted much attention in recent decades, which resulted in major fundamental advances in the chemistry of low oxidation state *p*-block compounds.[1–5] The interest in such type of systems arises from features of their unique electronic structure and chemical properties.[2,3,6–9]

To date, a variety of low-valent germanium compounds such as germylenes,[10–12] digermenes,[13,14] digermynes,[15,16] and Ge^I dimers[17–20] have been successfully isolated and structurally characterized. A reduction of the compounds mentioned above with strong reducing agents such as alkali metals, KC_8, *etc*., is a powerful tool for preparing substances possessing unusual properties.[21,22] For example, the reaction of tetraaryldigermene with lithium yields the rare heavy analogue of butadiene, *viz*. tetragermabuta-1,3-diene.[23,24] A treatment of organylhalogermylenes RGeHal with reductants results in Ge^I dimers,[17–20] or Ge-containing cyclopentadienide and cyclobutadiene-like dianion.[25] Recently, several reports on the 4π-antiaromatic heavy tetragermacyclobutadienes have been published.[26,27] An introduction of bulky amidinate substituents allowed the zwitterionic base-stabilized tetragermacyclobutadiene to be isolated.[26] A free cyclobutadiene germanium analogue has been recently obtained *via* the reaction of 1,2-dichlorodigermene bearing sterically-hindered hydrindacenyl groups with lithium naphthalenide.[27]

In 2015, Lee and Sekiguchi have demonstrated that the known dianion of R_3Si-substituted tetragermacyclobutadiene[28] can be successfully used for the preparation of heavy pyramidanes, in particular, pentagermapyramidane.[29] Pyramidane and its derivatives are the elusive and highly desirable targets that attract a great deal of attention due to their nonclassical structure and unusual bonding features.[30,31]

Among the family of divalent germanium compounds, N-heterocyclic germylenes represent one of the most studied class due to the possibility of variation of the substituents at heteroatoms and, therefore, fine tuning of their reactivity.[10–12] In contrast to N-heterocyclic germylenes, the chemistry of O,N-heterocyclic 10π-aromatic germylenes remains unexplored. There is only one Ge compound supported by a sterically hindered 4,6-di-*tert*-butyl-*N*-(2,6-diisopropylphenyl)-*o*-aminophenol ligand, but its molecular structure was not determined.[32]

Here we report the synthesis and structure of O,N-heterocyclic germylene **1** based on bulky 4,6-di-*tert*-butyl-*N*-*tert*-butyl-*o*-aminophenol chelating ligand (Bu^tApH_2) and the reaction of this germylene derivative with potassium in THF leading to the unique compound **2** comprising a conjugated Ge_4 chain.

Monomeric germylene complex **1** was obtained in 70% yield *via* the salt metathesis reaction (Scheme 1) between a dilithium derivative of the corresponding *o*-aminophenol[33] (Bu^tApLi_2) and $GeCl_2$·dioxane in THF. It is a pale-yellow crystalline compound possessing a high solubility in most organic solvents.[†] Compound **1** was found to be stable both in the solid state and in solutions under an inert atmosphere.

The molecular structure of compound **1** was determined by the single-crystal X-ray diffraction analysis (Figure 1).[‡]

[†] See Online Supplementary Materials for more details.

[‡] *Crystal data for* **1**. Pale yellow, $C_{18}H_{29}GeNO$ (0.200 × 0.130 × 0.110 mm), orthorhombic, space group *P*2(1)2(1)2(1), at 100 K: a = 9.6783(3), b = 10.0976(3) and c = 18.4011(5) Å, β = 90°, V = 1798.30(9) Å^3, Z = 4, d_{calc} = 1.285 g cm^{-3}, M_W = 348.01. 21119 reflections were collected (2.915–27.989°), absorption coefficient m = 1.703 mm^{-1}. Data/restraints/parameters: 4285/0/200. 4285 independent reflections (R_{int} = 0.0165). The final refinement parameters were: R_1 = 0.0160, wR_2 = 0.0430 for the reflections with $I > 2\sigma(I)$; R_1 = 0.0163, wR_2 = 0.0431 for all the reflections; largest diff. peak/hole was 0.361/–0.323 e Å^{-3}. GOF = 1.077.

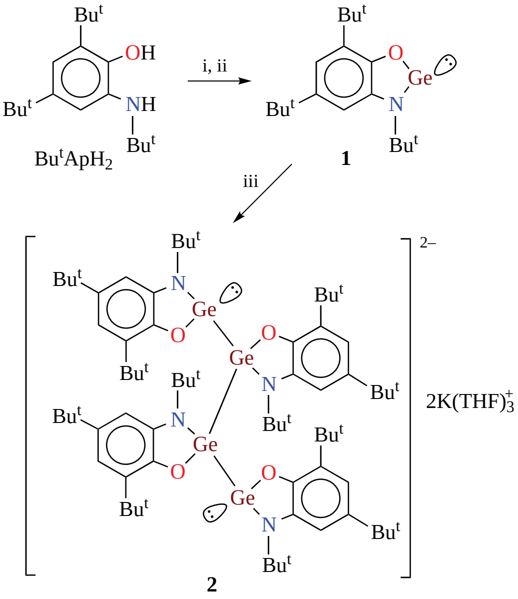

Scheme 1 *Reagents and conditions*: i, LiN(SiMe$_3$)$_2$ (2 equiv.); ii, GeCl$_2$·dioxane; iii, K (0.5 equiv.).

According to the X-ray diffraction data, compound **1** contains a dicoordinated germanium center located in its coordination sites occupied by O and N atoms of the organic ligand. The C(1)–O(1) and C(2)–N(1) distances [1.360(2) and 1.399(2) Å, respectively] are in the range typical of the dianionic form of such chelating ligand.[32–35] The C–C bonds in the six-membered carbon cycle (*ca.* 1.40 Å) of *o*-amidophenolate ligand are close to the typical aromatic ones. The Ge(1)–N(1) and Ge(1)–O(1) interatomic distances are comparable with those reported for the known N-heterocyclic-[10–12] and alkoxygermylenes.[36,37] The bite N(1)Ge(1)O(1) angle is also characteristic of such class of compounds.[10–12,36,37] It is necessary to note that germylene **1** does not contain intermolecular Ge–N or Ge–O bonds, which is characteristic of the relative tin(II)[34] and lead(II)[38] derivatives. An analysis of intermolecular interactions has revealed only the weak contacts between the Ge atom and π-system of the aromatic ring of adjacent molecule [Ge–arene contacts lie in the range of 3.579(2)–3.958(2) Å, Ge centre of 3.4831(7) Å] (Figure S1).

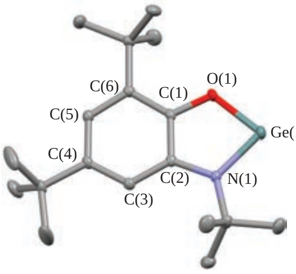

Figure 1 Structure of Bu^{t}ApGe **1** in solid state. Thermal ellipsoids are shown at the 50% probability level. Hydrogen atoms are omitted for clarity. Selected interatomic distances (Å): Ge(1)–O(1) 1.8289(11), Ge(1)–N(1) 1.8670(12), C(1)–O(1) 1.3602(18), C(2)–N(1) 1.3993(19), C(1)–C(6) 1.403(2), C(1)–C(2) 1.407(2), C(2)–C(3) 1.404(2), C(3)–C(4) 1.386(2), C(4)–C(5) 1.406(2), C(5)–C(6) 1.397(2). Selected bond angles (°): O(1)–Ge(1)–N(1) 86.18(5), C(1)–O(1)–Ge(1) 113.84(9), C(2)–N(1)–Ge(1) 112.17(10).

We attempted to reduce germylene **1** with potassium in THF at room temperature. It was found that the result of this reaction depends dramatically on the ratio of initial reagents. Thus, the reaction of **1** with K taken in 1 : 1 molar ratio proceeds with a colour change from the light yellow through blue to the intense dark brown. A deep reduction occurs in this case, followed by the consequent precipitation of amorphous germanium. On the other hand, using only 0.5 equiv. of potassium allowed us to stop the reaction at the 'blue' step. After concentration of the reaction mixture, dark blue-violet crystals of compound **2** were isolated in 46% yield (see Scheme 1). Complex **2** was found to be extremely sensitive to air.

Single crystal X-ray diffraction analysis has revealed a novel germanium complex (Bu^{t}Ap)$_4$Ge$_4$K$_2$(THF)$_6$ (**2**) comprising a unique Ge$_4$ skeleton. Figure 2 shows its molecular structure in the solid state. All metrical data for chelating *o*-amidophenolate moieties in **2** such as C–O, C–N and C–C bond lengths are quite close to those in the starting compound **1** and confirm a dianionic[19–21] nature of the ligands. The Ge–N and Ge–O bonds for the edge Ge(1) atoms are shortened as compared to the central Ge(2), which is expected to cause an increased coordination number of the latter. All the Ge–O and Ge–N bonds in **2** are significantly longer as compared to the related distances in **1**.

The practically planar Ge$_4$ chain [the deviation for all Ge atoms from Ge(1)–Ge(4) plane is only 0.19 Å] in **2** contains three Ge–Ge bonds: Ge(1)–Ge(2) distances are equal to 2.7088(2) Å, while Ge(2)–Ge(2A) is quite close to them [2.6690(3) Å]. These interatomic Ge–Ge distances are in the far edge of range that is typical of the known Ge^I–Ge^I bonds.[4] Potassium ions in **2** are bonded with three THF molecules and η^5-coordinated by the central {CCOGeN} metallocycle. These moieties are not planar in contrast to the peripherical ones. The bending angle along O(2)···N(2) line is 17.73°.

In order to shed light on the nature of Ge–Ge interactions, DFT calculations were performed for compound **2**. Its geometry was optimized at the CAM-B3LYP/dgdzvp[39] level of theory using the Gaussian 09 software package.[40] The optimized structure was in a good agreement with the X-ray diffraction data, although with slightly overestimated Ge–Ge bond lengths. According to the natural bond orbital (NBO)[41] analysis, there are some key bonding interactions in **2**. The Ge(2)–Ge(2A) bond derived largely from Ge *p* orbital overlap (5.6% *s*, 94% *p*) is exclusively *σ* in character similarly to the Si^I or Ge^I dimers

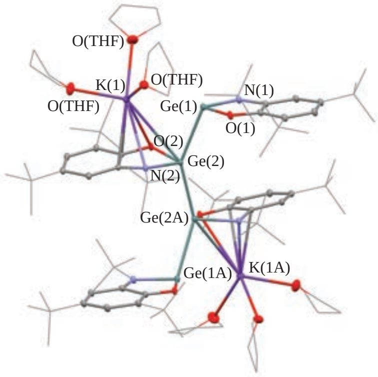

Figure 2 Structure of (Bu^{t}Ap)$_4$Ge$_4$K$_2$(THF)$_6$ **2** in solid state. Thermal ellipsoids are shown at the 30% probability level for the key atoms. Hydrogen atoms are omitted for clarity. Selected interatomic distances (Å): Ge(1)–O(1) 1.8601(8), Ge(1)–N(1) 1.8988(10), Ge(1)–Ge(2) 2.7088(2), Ge(2)–Ge(2A) 2.6690(3), Ge(2)–O(2) 1.8857(8), Ge(2)–N(2) 1.9382(9). Selected bond angle: Ge(2A)–Ge(2)–Ge(1) 145.904(7)°.

Crystal data for **2**. Blue-violet, C$_{96}$H$_{164}$Ge$_4$K$_2$N$_4$O$_{10}$ (0.846 × 0.757 × 0.411 mm), monoclinic, space group *C*$_2$/*c*, at 100 K: a = 35.0133(8), b = 12.05010(10) and c = 30.1745(7) Å, β = 127.731(4)°, V = 10068.9(5) Å^3, Z = 4, d_{calc} = 1.255 g cm^{-3}, M_W = 1902.86. 101330 reflections were collected (3.188–30.508°), absorption coefficient m = 1.320 mm^{-1}. Data/restraints/parameters: 15325/45/558. 15325 independent reflections (R_{int} = 0.0249). The final refinement parameters were: R_1 = 0.0253, wR_2 = 0.0588 for the reflections with $I > 2\sigma(I)$; R_1 = 0.0333, wR_2 = 0.0636 for all the reflections; largest diff. peak/hole was 0.593/–0.429 e Å^{-3}. GOF = 1.065.

isolated earlier.[17–20] In addition to the principal Ge(2)–Ge(2A) bonding, we have observed a significant dative Ge(2)LP → *p*-Ge(1) and Ge(2A)LP → *p*-Ge(1A) interactions involving lone pairs of electrons of the central germanium Ge(2,2A) and vacant orbitals of peripheral Ge(1,1A) atoms with a high *p*-character. Orbital occupancy in all the cases is more than 1.8 electrons per bond. Moreover, the donor–acceptor interaction of Ge(1,1A) LP with the Ge(2)–Ge(2A) σ* orbital was observed, which, however, did not lead to the double bonds between Ge(1)–Ge(2) and Ge(1A)–Ge(2A) atoms due to its weakness. Donation of electronic density to the σ* orbital should weaken this bond and consequently make it longer. Especially there is more sterical pressure on the central Ge(2)–Ge(2A) bond than on the adjacent Ge(1)–Ge(2) bonds. This leads to an alignment of σ bonds with two different characters in compound **2** and shifts the bond lengths to the far edge of region characteristic of the $\mathrm{Ge^I}$–$\mathrm{Ge^I}$ species.

Distribution of Mulliken charges on the Ge atoms in the $\mathrm{Ge_4}$ framework differs insignificantly: +0.42 and +0.32 for Ge(2,2A) and Ge(1,1A), respectively.

Figure 3 shows the canonical molecular orbitals (CMOs) for **2**. The HOMO can be described as a Ge(2)–Ge(2A) σ bond mainly composed by Ge *p* orbitals and is comparable with the shape of CMOs calculated for a series of $\mathrm{Si^I}$ and $\mathrm{Ge^I}$ dimers.[17–20] HOMO-10 is responsible for an orbital interaction involving LP from peripheral Ge atoms and Ge(2)–Ge(2A) σ* orbital leading to an additional stabilization of the $\mathrm{Ge_4}$-core. Considerable conjugation and delocalization of the electron density appear as a consequence of this backbonding. HOMO-13 and HOMO-14 demonstrate Ge(2)LP → *p*-Ge(1) and Ge(2A)LP → *p*-Ge(1A) σ bonds, respectively.

We have attempted to calculate the energetic aspects of dissociation of **2** through the breaking of the central Ge(2)–Ge(2A) bond into two paramagnetic dimers of the general formula $[\mathrm{Bu^tApGe{-}GeApBu^t}]^{\bullet-}\mathrm{K^+}$. Since the bond dissociation is accompanied with changing the multiplicity of the system, we have calculated the MECP (minimum energy crossing point, a point that has a minimal energy on the seam lying on the crossing of two potential energy surfaces of different multiplicity),[42] which is known as an analogue of the transition state in the case of closed- shell molecules. It was found that the estimated barrier (25.3 kcal $\mathrm{mol^{-1}}$) for Ge(2)–Ge(2A) bond breaking lowers a probability of this process in solution at ambient temperatures (Figure S10). It was confirmed by the absence of EPR signals for compound **2** in both the solid state and solution. Nevertheless, **2** was not stable in its tetrameric form in diluted solution. Our preliminary experiments have revealed that there is a dynamic equilibrium including apparently a dissociation of at least one of the peripheral germylenes. This was also indicated by the effect of compound **2** concentration on its solution colour. Deep blue crystals gave the deep blue concentrated solution. The colour of the latter reversibly changed by wine-red under its dilution. Moreover, compound **2** decomposed under its dissolution in toluene. The detailed study of behaviour of compound **2** solution is the subject of our ongoing investigations.

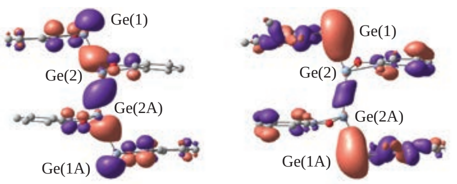

HOMO (–2.79 eV)　　HOMO-10 (–6.49 eV)

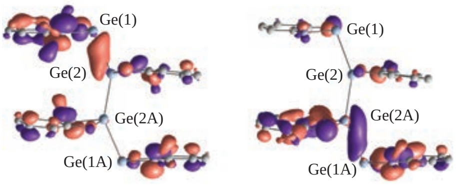

HOMO-13 (–6.96 eV)　　HOMO-14 (–7.05 eV)

Figure 3 Selected canonical molecular orbitals with shown orbital energies for compound **2**. Isovalue is 0.04 a.u. Hydrogen atoms, $\mathrm{Bu^t}$ substituents, and $\mathrm{K^+}$ counterions are omitted for clarity.

Taking into account the acquired data, we can assume a possible mechanism for the reduction of germylene **1** with potassium at their 1 : 0.5 molar ratio (Scheme S1). At the initial step, an electron transfer from potassium to the aromatic metallacycle occurs producing a radical-ionic (*S* = 1/2) intermediate $[\mathrm{Bu^tApGe}]^{\bullet-}\mathrm{K^+}$. According to the DFT calculations, spin density in this radical is mainly localized at the *p* orbital of Ge center (q_s^{Ge} = 0.825) that is in a good agreement with the fact that LUMO of initial germylene **1** is mostly *p* orbital (Figure S11). $\mathrm{Ge^I}$-centered radical $[\mathrm{Bu^tApGe}]^{\bullet-}\mathrm{K^+}$ is unstable and reacts rapidly with starting compound **1** to give a paramagnetic $\mathrm{Ge_2}$ specie that was detected by EPR spectroscopy. The EPR spectrum of reaction mixture contains a weak signal characteristic of *S* = 1/2 species (Figure S2). This signal is moderately resolved at 285 K and shows a hyperfine structure due to the coupling of unpaired electron with two equivalent ^{14}N and two equivalent ^{1}H nuclei. The hyperfine coupling constants are $a_i(^{14}\mathrm{N})$ = 0.156 mT (2N), $a_i(^{1}\mathrm{H})$ = 0.166 mT (2H), and g_i = 1.9987. Unfortunately, the weak signal did not allow us to observe any satellite splitting on the magnetic isotope ^{73}Ge. The similar pattern in EPR spectra was reported for a monoradical complex of germanium[32] bearing two related amidophenolate ligands. Obviously, the small hyperfine splitting constants on N and H nuclei in the observed paramagnetic specie indicate that the spin density is predominantly concentrated on the Ge atoms. It is also evidenced by a low value of the *g* factor characteristic of Ge-centered radicals.[22] The acquired data allowed us to assign the observed spectrum to $[\mathrm{Bu^tAPGe{-}GeAPBu^t}]^{\bullet-}$ specie. The last one dimerizes to give the title compound **2**, *viz.* $(\mathrm{Bu^tAp})_4\mathrm{Ge_4K_2(THF)_6}$, comprising the unusual $\mathrm{Ge_4}$ skeleton.

In summary, new 3,5,7-tri-*tert*-butyl-1,3,2-benzoxazagermol-2-ylidene **1** was synthesized. It is monomeric in solid state and demonstrates weak Ge–arene intermolecular interactions in crystals. The reduction of this O,N-heterocyclic germylene with potassium in THF was accompanied with the formation of unusual low-valent germanium compound **2**, $(\mathrm{Bu^tAp})_4\mathrm{Ge_4K_2(THF)_6}$, consisting of the unique $\mathrm{Ge_4}$ chain. The detailed investigations of electron density distribution in **2** has been performed using quantum-chemical calculations, which revealed a variety of bonding interactions inside the $\mathrm{Ge_4}$ framework. There are three σ bonds of different characters (covalent and dative) between the Ge atoms together with an orbital interaction involving LP from the peripheral Ge atoms and Ge(2)–Ge(2A) σ* orbital. A significant conjugation in the entire $\mathrm{Ge_4}$ framework leads to a delocalization of the electron density over the four Ge atoms and equalization of the Ge–Ge distances giving rise to the uniform 10e4c system.

This work was supported by the Russian Science Foundation (grant no. 17-13-01428). The study was performed using an equipment of the Analytical Center at the G. A. Razuvaev Institute of Organometallic Chemistry of the Russian Academy of Sciences.

Online Supplementary Materials

Supplementary data associated with this article can be found in the online version at doi: 10.1016/j.mencom.2020.03.025.

References

1 Y. Mizuhata, T. Sasamori and N. Tokitoh, *Chem. Rev*., 2009, **109**, 3479.
2 V. Ya. Lee and A. Sekiguchi, in *Organometallic Compounds of Low-Coordinate Si, Ge, Sn and Pb: From Phantom Species to Stable Compounds*, Wiley, Chichester, UK, 2010, pp. 199–334.
3 E. Rivard, *Chem. Soc. Rev*., 2016, **45**, 989.
4 M. Asay, C. Jones and M. Driess, *Chem. Rev*., 2011, **111**, 354.
5 R. C. Fischer and P. P. Power, *Chem. Rev*., 2010, **110**, 3877.
6 P. P. Power, *Acc. Chem. Res*., 2011, **44**, 627.
7 M. L. McCrea-Hendrick, C. A. Caputo, J. Linnera, P. Vasko, C. M. Weinstein, J. C. Fettinger, H. M. Tuononen and P. P. Power, *Organometallics*, 2016, **35**, 2759.
8 P. P. Power, *Nature*, 2010, **463**, 171.
9 J. Turek, B. Braïda and F. De Proft, *Chem.–Eur. J.*, 2017, **23**, 14604.
10 R. R. Aysin, L. A. Leites, S. S. Bukalov, A. V. Zabula and R. West, *Inorg. Chem.*, 2016, **55**, 4698.
11 L. A. Leites, S. S. Bukalov, R. R. Aysin, A. V. Piskunov, M. G. Chegerev, V. K. Cherkasov, A. V. Zabula and R. West, *Organometallics*, 2015, **34**, 2278.
12 S. K. Liew, S. M. I. Al-Rafia, J. T. Goettel, P. A. Lummis, S. M. McDonald, L. J. Miedema, M. J. Ferguson, R. McDonald and E. Rivard, *Inorg. Chem.*, 2012, **51**, 5471.
13 N. Hayakawa, T. Sugahara, Y. Numata, H. Kawaai, K. Yamatani, S. Nishimura, S. Goda, Y. Suzuki, T. Tanikawa, H. Nakai, D. Hashizume, T. Sasamori, N. Tokitoh and T. Matsuo, *Dalton Trans.*, 2018, **47**, 814.
14 L. Pu, A. D. Phillips, A. F. Richards, M. Stender, R. S. Simons, M. M. Olmstead and P. P. Power, *J. Am. Chem. Soc.*, 2003, **125**, 11626.
15 Y. Peng, R. C. Fischer, W. A. Merrill, J. Fischer, L. Pu, B. D. Ellis, J. C. Fettinger, R. H. Herber and P. P. Power, *Chem. Sci.*, 2010, **1**, 461.
16 Y. Sugiyama, T. Sasamori, Y. Hosoi, Y. Furukawa, N. Takagi, S. Nagase and N. Tokitoh, *J. Am. Chem. Soc.*, 2006, **128**, 1023.
17 J. Li, C. Schenk, C. Goedecke, G. Frenking and C. Jones, *J. Am. Chem. Soc.*, 2011, **133**, 18622.
18 C. Jones, S. J. Bonyhady, N. Holzmann, G. Frenking and A. Stasch, *Inorg. Chem.*, 2011, **50**, 12315.
19 M. L. Bin Ismail, F.-Q. Liu, W.-L. Yim, R. Ganguly, Y. Li and C.-W. So, *Inorg. Chem.*, 2017, **56**, 5402.
20 D. Nieder, L. Klemmer, Y. Kaiser, V. Huch and D. Scheschkewitz, *Organometallics*, 2018, **37**, 632.
21 J. A. Kelly, M. Juckel, T. J. Hadlington, I. Fernández, G. Frenking and C. Jones, *Chem. – Eur. J.*, 2019, **25**, 2773.
22 W. D. Woodul, E. Carter, R. Müller, A. F. Richards, A. Stasch, M. Kaupp, D. M. Murphy, M. Driess and C. Jones, *J. Am. Chem. Soc.*, 2011, **133**, 10074.
23 H. Schäfer, W. Saak and M. Weidenbruch, *Angew. Chem., Int. Ed.*, 2000, **39**, 3703.
24 G. Ramaker, A. Schäfer, W. Saak and M. Weidenbruch, *Organometallics*, 2003, **22**, 1302.
25 W. Wang, S. Yao, C. van Wüllen and M. Driess, *J. Am. Chem. Soc.*, 2008, **130**, 9640.
26 H.-X. Yeong, H.-W. Xi, Y. Li, S. B. Kunnappilly, B. Chen, K.-C. Lau, H. Hirao, K. H. Lim and C.-W. So, *Chem. – Eur. J.*, 2013, **19**, 14726.
27 K. Suzuki, Y. Numata, N. Fujita, N. Hayakawa, T. Tanikawa, D. Hashizume, K. Tamao, H. Fueno, K. Tanaka and T. Matsuo, *Chem. Commun*., 2018, **54**, 2200.
28 V. Ya. Lee, Y. Ito, H. Yasuda, K. Takanashi and A. Sekiguchi, *J. Am. Chem. Soc.*, 2011, **133**, 5103.
29 V. Ya. Lee, Y. Ito, O. A. Gapurenko, A. Sekiguchi, V. I. Minkin, R. M. Minyaev and H. Gornitzka, *Angew. Chem., Int. Ed.*, 2015, **54**, 5654.
30 V. Ya. Lee, Y. Ito, A. Sekiguchi, H. Gornitzka, O. A. Gapurenko, V. I. Minkin and R.M. Minyaev, *J. Am. Chem. Soc.*, 2013, **135**, 8794.
31 V. Ya. Lee, O. A. Gapurenko, Y. Ito, T. Meguro, H. Sugasawa, A. Sekiguchi, R. M. Minyaev, V. I. Minkin, R. H. Herber and H. Gornitzka, *Organometallics*, 2016, **35**, 346.
32 A.V. Piskunov, I. A. Aivaz'yan, A. I. Poddel'sky, G. K. Fukin, E. V. Baranov, V. K. Cherkasov and G. A. Abakumov, *Eur. J. Inorg. Chem.*, 2008, 1435.
33 M. G. Chegerev, A. V. Piskunov, A. A. Starikova, S. P. Kubrin, G. K. Fukin, V. K. Cherkasov and G. A. Abakumov, *Eur. J. Inorg. Chem.*, 2018, 1087.
34 M. G. Chegerev, A. V. Piskunov, K. V. Tsys, A. G. Starikov, K. Jurkschat, E. V. Baranov, A. I. Stash and G. K. Fukin, *Eur. J. Inorg. Chem.*, 2019, 875.
35 M. G. Chegerev, A. V. Piskunov, A. V. Maleeva, G. K. Fukin and G. A. Abakumov, *Eur. J. Inorg. Chem.*, 2016, 3813.
36 N. N. Zemlyansky, I. V. Borisova, V. N. Khrustalev, M. Yu. Antipin, Y. A. Ustynyuk, M. S. Nechaev and V. V. Lunin, *Organometallics*, 2003, **22**, 5441.
37 P. Kitschke, L. Mertens, T. Rüffer, H. Lang, A. A. Auer and M. Mehring, *Eur. J. Inorg. Chem*., 2015, 4996.
38 K. V. Tsys, M. G. Chegerev, G. K. Fukin and A. V. Piskunov, *Mendeleev Commun.*, 2018, **28**, 527.
39 T. Yanai, D. P. Tew and N. C. Handy, *Chem. Phys. Lett*., 2004, **393**, 51.
40 M. J. Frisch, G. W. Trucks, H. B. Schlegel, G. E. Scuseria, M. A. Robb, J. R. Cheeseman, G. Scalmani, V. Barone, B. Mennucci, G. A. Petersson, H. Nakatsuji, M. Caricato, X. Li, H. P. Hratchian, A. F. Izmaylov, J. Bloino, G. Zheng, J. L. Sonnenberg, M. Hada, M. Ehara, K. Toyota, R. Fukuda, J. Hasegawa, M. Ishida, T. Nakajima, Y. Honda, O. Kitao, H. Nakai, T. Vreven, J. A. Montgomery, Jr., J. E. Peralta, F. Ogliaro, M. Bearpark, J. J. Heyd, E. Brothers, K. N. Kudin, V. N. Staroverov, R. Kobayashi, J. Normand, K. Raghavachari, A. Rendell, J. C. Burant, S. S. Iyengar, J. Tomasi, M. Cossi, N. Rega, J. M. Millam, M. Klene, J. E. Knox, J. B. Cross, V. Bakken, C. Adamo, J. Jaramillo, R. Gomperts, R. E. Stratmann, O. Yazyev, A. J. Austin, R. Cammi, C. Pomelli, J. W. Ochterski, R. L. Martin, K. Morokuma, V. G. Zakrzewski, G. A. Voth, P. Salvador, J. J. Dannenberg, S. Dapprich, A. D. Daniels, Ö. Farkas, J. B. Foresman, J. V. Ortiz, J. Cioslowski and D. J. Fox, *GAUSSIAN 09, Revision D.01*, Gaussian, Wallingford, CT, 2013.
41 E. D. Glendening, J. K. Badenhoop, A. E. Reed, J. E. Carpenter, J. A. Bohmann, C. M. Morales, C. R. Landis and F. Weinhold, *NBO PROGRAM 6.0, Natural Bond Orbital Analysis Programs*, Madison, WI, 2013.
42 J. N. Harvey, M. Aschi, H. Schwarz and W. Koch, *Theor. Chem. Acc.*, 1998, **99**, 95.

Received: 23rd August 2019; Com. 19/6017